Phytopathology Research

RESEARCH

Open Access

Nothophoma spp. causing leaf blight of ancient *Platycladus orientalis*

Ning Jiao[1], Jiawen Wang[1], Zhe Zhang[1] and Ying Zhang[1*]

Abstract

Ancient *Platycladus orientalis* holds significant ecological, landscape, historical, and cultural value. In northern China, leaf blight has significantly impacted the growth and ornamental value of ancient *P. orientalis*. In this study, 26 blight leaf samples of ancient *P. orientalis* were collected in Beijing, China. Phylogenetic analysis based on the concatenated internal transcribed spacer (ITS), β-tubulin (*tub*2), and RNA polymerase second largest subunit (*rpb*2) DNA sequence data combined with fungal morphological characteristics revealed three taxa of *Nothophoma*, i.e. *N. platycladus*, *N. spiraeae*, and *N. juglandis*. Of which, *N. platycladus* is a species new to science. Koch's postulates indicated that all these three species of *Nothophoma* could cause leaf blight of *P. orientalis*.

Keywords Ancient trees, Plant pathogens, Phylogeny, Taxonomy, Koch's postulates

Background

Ancient trees are ecologically significant groups that play important roles in supporting the natural community structure and dynamics (Liu et al. 2019). They can enhance ecosystem services, including maintaining water balance, promoting carbon sequestration, and improving air quality as well as having high landscape, historical and cultural value (Blicharska and Mikusiński 2014; Lindenmayer and Laurance 2017; Wan et al. 2020). The *Platycladus orientalis* (*Platycladus*, Cupressaceae), an evergreen tree with significant medicinal value, is native to China and North Korea (Li et al. 2023). There are 39,408 ancient trees in Beijing, with ancient *P. orientalis* accounting for 19% (Chen 2010). The ancient *P. orientalis*, symbolizing auspiciousness and longevity due to its robust vitality and long lifespan, is commonly found in prominent historical and cultural sites such as palaces, parks, and temples in China (Huang et al. 2021).

*Correspondence:
Ying Zhang
yzhang@bjfu.edu.cn
[1] School of Ecology and Nature Conservation, Beijing Forestry University, Beijing 100083, China

Leaf blight is the most common disease of *P. orientalis* in China, significantly impacting plant growth and landscape aesthetics (Zheng et al. 2022). Early to 1922, *P. orientalis* leaf blight caused by *Alternaria pruni* was identified in China (Zhu 1922). Subsequently, *Keithia thujina* was recognized as the causal agent of the *P. orientalis* leaf blight in Xiangshan Park, Beijing (Zhao 1978). *Monochaetia* sp. was reported to cause *P. orientalis* leaf blight in Hanwangshan Forest Farm, Yang County, Shaanxi Province (Jiang et al. 1984). Dai et al. (1992) discovered that *Chloroscypha platycladus* caused leaf blight of *P. orientalis* in the hilly areas of southern China. The study on leaf blight of ancient *P. orientalis* in Mausoleum of Yellow Emperor of Shaanxi showed that *Alternaria alternata* and *Pestalotiopsis paeoniicola* were the causal agent in this area (Li et al. 2021). Due to the over-mature stage of ancient trees, their physiological functions decline, stress resistance decreases, and the probability of disease infection significantly increases (Chen 2014). This phenomenon is particularly noticeable in ancient *P. orientalis*. However, the study on ancient *P. orientalis* disease is still quite scarce.

We recently investigated the diseases of ancient *P. orientalis*. During the investigation of the ancient *P. orientalis* in Beijing, approximately half of the plants were

suffered from leaf blight. In this study, blight leaves of ancient *P. orientalis* were collected from four scenic areas in Beijing, and 20 fungal isolates were obtained. The aim of this study is to 1) identify the fungal isolates based on morphological characteristics and multigene phylogenetic analysis, and 2) evaluate their pathogenicity by applying Koch's postulates.

Results

Phylogenetic analysis

The isolates of *Nothophoma* (including seven isolates: CGMCC3.27066, CGMCC3.27067, CGMCC3.27068, CGMCC3.27069, CGMCC3.27070, CGMCC3.27071, and CGMCC3.27072) from ancient *P. orientalis* blight leaves were identified as a new species and two known species based on an analysis of concatenated ITS, *tub*2, and *rpb*2 sequence dataset composed of 39 isolates of *Nothophoma* species and *Phoma herbarum* (CBS 615.75) as an outgroup taxon (Table 1). A total of 1491 characters with 179 parsimony-informative characters were obtained in the phylogenetic analysis. The heuristic search with random addition of taxa (1000 replicates) generated 5000 most parsimonious trees (Length = 492, Consistency index = 0.628, Retention index = 0.781, Rescaled consistency = 0.491, and Homoplasy index = 0.372). Through three analyses (Maximum likelihood ML, Bayesian inference BI, and Maximum parsimony MP), this new species (the strains CGMCC3.27069, CGMCC3.27070, and CGMCC3.27071) was introduced based on the molecular data, indicating that it is a distinct clade with well support (ML/BI/MP = 83/1/82) and it is closely related to *Nothophoma pruni* (Fig. 1). The strains CGMCC3.27072 and CGMCC3.27066 were co-clustered into the clade of *Nothophoma spiraeae* according to the multi-locus phylogeny. The strains CGMCC3.27067 and CGMCC3.27068 belong to *Nothophoma juglandis* by the multi-locus phylogeny assays. Furthermore, only the tree shape of ML is presented here, with ML, BI, and MP values plotted on the branches.

Taxonomy

Nothophoma platycladus Y. Zhang ter & N. Jiao, sp. nov. (Fig. 2).

Mycobank No: 853425.

Etymology: In reference to the genus of the host name, *Platycladus*.

Description: Sexual morph was not observed. Asexual morph was developed on malt extract agar (MEA). Conidiomata pycnidial, semi-immersed or superficial on the agar surface, spherical to irregular, mostly aggregated, solitary or confluent, glabrous, thick-walled, with hypha around the pycnidial, 301–545 × 236–456 µm (mean SD = 438 ± 84 × 331 ± 66 µm, *n* = 20), dark brown, gradually with age turning black, eventually forming small black spots (Fig. 2c). Ostioles single, central, papillate or elongated to a neck, aperture 43–74 µm (mean SD = 56 ± 14 µm, *n* = 20) (Fig. 2d). Pycnidial wall pseudoparenchymatous, composed of isodiametric cells, 3–6 layers, 22–46 µm thick, outer wall 2–3 layers, and pigmented. Conidiogenous cells phialidic, hyaline, smooth, ampulliform to doliiform, 4.0–6.5 × 2.5–4.5 µm (mean SD = 5.0 ± 1.5 × 3.5 ± 1.0 µm, *n* = 20) (Fig. 2e). Conidia hyaline but incidentally olivaceous buff, ovoid or ellipsoidal, smooth and thin-walled, aseptate, 4.7–6.4 × 2.8–4.3 µm (mean SD = 5.2 ± 0.5 × 3.7 ± 0.4 µm, *n* = 50), sometimes with some very small guttules (Fig. 2f, g).

Culture characteristics: Colonies on MEA, 42 to 48 mm in diameter after 7 days at 26°C, colony edges are regular, nearly round, aerial mycelium flat, dark brown to black in center, and have white mycelium on the edges, reversing pale black in center, and darkened gradually after 10 days. Colonies were dense and fluffy, with abundant pycnidia, irregular distribution on the surface of the medium, which produce conidial matrix drop (Fig. 2a, b).

Additional specimens examined: China, Beijing, Chaoyang District, Ritan Park, from blight leaf of ancient *Platycladus orientalis*, 20 September 2023, Y. Zhang and N. Jiao (holotype HMAS 352975; ex-type living culture CGMCC3.27069). China, Beijing, Chaoyang District, Ritan Park, from blight leaf of ancient *P. orientalis*, 20 September 2023, Y. Zhang and N. Jiao (Paratype HMAS 352976; living culture CGMCC3.27070). China, Beijing, Xicheng District, Beihai Park, from blight leaf of ancient *P. orientalis*, 25 September 2023, Y. Zhang and N. Jiao (Paratype HMAS 352977; living culture CGMCC3.27071).

Notes: On the phylogram, *Nothophoma platycladus* is closely related but sibling to *Nothophoma brennandiae*, *Nothophoma spiraeae*, *Nothophoma quercina*, *Nothophoma juglandis*, and *Nothophoma pruni* (Fig. 1). Morphologically, the conidia of *N. platycladus* have a darker color and smaller aspect ratio compared to those of *N. pruni* (5.2 × 3.7; L/W = 1.4 vs. 6.0 × 3.3; L/W = 1.8 µm) (Fig. 2f, g). Morphological characteristics and multi-locus phylogenetic analysis indicated that *N. platycladus* is a novel species of *Nothophoma*. *Nothophoma multilocularis* without available DNA sequence was eliminated from the phylogenetic tree (http://www.indexfungorum.org.asp, April 11, 2024). *N. platycladus* can be clearly distinguished from *Nothophoma multilocularis* in terms of the conidium dimension (4.7–6.4 × 2.7–4.3 vs. 9–20 × 3–4 µm) (Fig. 2f, g) (Abdel-Wahab et al. 2017).

Nothophoma spiraeae L. X. Zhang, T. Yin, M. Pan, C. M. Tian, and X. L. Fan, Phytotaxa 430:150, (2020) (Fig. 3).

Table 1 Isolates and GenBank accession numbers used in this study[a]

Species	Strain	Host	Country	GenBank accession number[b]		
				ITS	*tub*2	*rpb*2
Nothophoma acaciae	CBS 143404	*Acacia melanoxylon*	Australia	MG386056.1	MG386167.1	MG386144.1
Nothophoma arachidis	CBS 125.93	*Arachis hypogaea*	India	GU237771	GU237583	KT389656
Nothophoma anigozanthi	CBS 381.91	*Anigozanthus maugleisii*	Netherlands	GU237852	GU237580	KT389655
Nothophoma brennandiae	CBS 262.95	*Olea europaea*	Italy	MN973554.1	MT005657.1	MT018198.1
Nothophoma brennandiae	CBS 125540	*Ostrya carpinifolia*	Italy	MN973555.1	MT005658.1	MT018199.1
Nothophoma brennandiae	CBS 140540	House dust	Canada	MN973557.1	MT005660.1	MT018201.1
Nothophoma chromolaenae	MFLUCC 17–1443	*Chromolaena odorata*	Thailand	MT214364.1	N/A	N/A
Nothophoma eucalyptigena	CBS 142535	*Eucalyptus* sp.	Australia	KY979771	KY979935.1	KY979852
Nothophoma garlbiwalawarda	BRIP 69587	*Senna artemisioides*	Australia	MN567684.1	N/A	MN604935.1
Nothophomaga rlbiwalawarda	BRIP 69594	*Senna artemisioides*	Australia	MN567685.1	N/A	MN604936.1
Nothophomaga rlbiwalawarda	BRIP 69595	*Senna artemisioides*	Australia	MN567686.1	N/A	MN604937.1
Nothophoma gossypiicola	CBS 377.67	*Gosssypium* spp.	USA	GU237845	GU237611	KT389658
Nothophoma infossa	CBS 123395	*Fraxinus pennsylvanica*	Argentina	FJ427025	FJ427135	KT389659
Nothophoma infuscata	CBS 121931	*Acacia longifolia*	New Zealand	MN973559.1	MT005662.1	MT018203.1
Nothophoma juglandis	CGMCC3.23563	*Juglans regia*	China	MZ519403	MZ570583	MZ502664
Nothophoma juglandis	CGMCC3.23564	*Juglans regia*	China	MZ519404	MZ570584	MZ502665
Nothophoma juglandis	CGMCC3.23565	*Juglans regia*	China	MZ519405	MZ570585	ME502666
Nothophoma juglandis	**CGMCC3.27067**	***Platycladus orientalis***	**China**	**PP600106**	**PP595989**	**PP595982**
Nothophoma juglandis	**CGMCC3.27068**	***Platycladus orientalis***	**China**	**PP600107**	**PP595990**	**PP595983**
Nothophoma macrospora	UTHSC DI16-276	Human respiratory tract	USA	LN880536	LN880539	LT593073
Nothophoma ngayawang	BRIP 69582	*Senna artemisioides*	Australia	MN567688.1	N/A	MN604939.1
Nothophoma naiawu	BRIP 69583	*Senna artemisioides*	Australia	MN567687.1	N/A	MN604938.1
Nothophoma nullicana	CPC 32330	*Acacia falciformis*	Australia	MG386054.1	MG386165.1	MG386143.1
Nothophoma prosopidis	CPC 21701	*Prosopis* sp.	South Africa	KF777150.1	N/A	N/A
Nothophoma prosopidis	CPC 21705	*Prosopis* sp.	South Africa	KF777152.1	N/A	N/A
Nothophoma pruni	MFLUCC 18–1600	*Prunus avium*	China	MH827007	MH853671	MH853664
Nothophoma platycladus	**CGMCC3.27069**	***Platycladus orientalis***	**China**	**PP600101**	**PP595984**	**PP595977**
Nothophoma platycladus	**CGMCC3.27071**	***Platycladus orientalis***	**China**	**PP600103**	**PP595986**	**PP595979**
Nothophoma platycladus	**CGMCC3.27070**	***Platycladus orientalis***	**China**	**PP600102**	**PP595985**	**PP595978**
Nothophoma quercina	CBS 633.92	*Microsphaera alphitoides*	Ukraine	GU237900	GU237609	KT389657
Nothophoma raii	MCC 1082	Soil	India	MF664467	MF664468	N/A
Nothophoma spiraeae	CFCC 53928	*Spiraea salicifolia*	China	MN737833	MN879295	MN879292
Nothophoma spiraeae	CFCC 53929	*Spiraea salicifolia*	China	MN737834	MN879296	MN879293
Nothophoma spiraeae	CFCC 53930	*Spiraea salicifolia*	China	MN737832	MN879297	MN879294
Nothophoma spiraeae	**CGMCC3.27072**	***Platycladus orientalis***	**China**	**PP600104**	**PP595987**	**PP595980**
Nothophoma spiraeae	**CGMCC3.27066**	***Platycladus orientalis***	**China**	**PP600105**	**PP595988**	**PP595981**
Nothophoma taboriae	BRIP 71522a	Myrtaceae	Australia	OP599628	N/A	OP627086
Nothophoma variabilis	UTHSC DI16-285	Human respiratory tract	USA	LT592939	LT593008	LT593078
Phoma herbarum	CBS 615.75	*Rosa multiflora* cv. Cathayensis	Netherlands	FJ427022	KF252703	KP330420

*rpb*2 RNA polymerase second largest subunit, *tub*2 β-tubulin, N/A not available

[a] Newly generated sequences are indicated in bold

[b] ITS, internal transcribed spacer

Description: Sexual morph was not observed. Asexual morph: Pycnidia is solitary or aggregated, globose to subglobose, glabrous, olivaceous buff, superficial on or semi-immersed in agar (Fig. 3a, b), Conidia are hyaline, occasionally olive, ovoid, smooth, thin-walled, aseptate, 5.0–7.5 × 2.8–4.8 μm (mean SD = 6.3 ± 1.0 × 3.9 ± 0.5 μm, $n = 50$) (Fig. 3f, g).

Culture characteristics: Colonies on MEA, 52 to 59 mm in diameter after 7 days at 26°C, the cultures initially appeared hazel and flat, with a thick texture in the

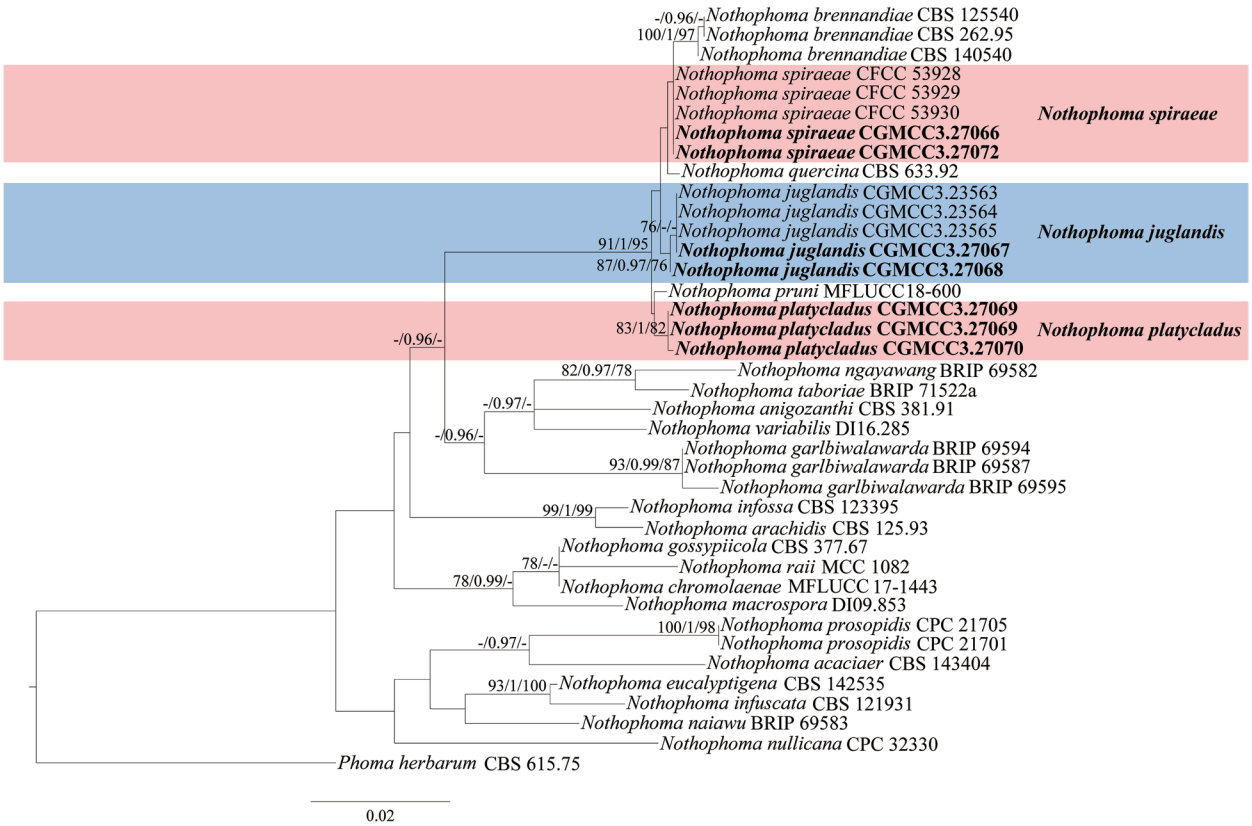

Fig. 1 Phylogenetic tree of Maximum Likelihood analyses of *Nothophoma* based on combined ITS, *tub*2, and *rpb*2 genes. Designated outgroup taxa is *Phoma herbarum* (CBS 615.75). RAxML bootstrap support values (ML ≥ 75%), Bayesian posterior probability (PP ≥ 0.95), and Maximum parsimony bootstrap support values (MP ≥ 75%) are shown in nodes (ML/PP/MP). The scale bar shows 0.02 changes

center and a thin texture surrounding it after 3 days. Of 7 to 10 days, they were gradually darkened. The colonies were dense and fluffy, showing abundant pycnidia irregularly distributed on the medium's surface, along with the production of a creamy white conidial matrix drop (Fig. 3a, b).

Additional specimens examined: China, Beijing, Dongcheng District, Zhongshan Park, from blight leaf of ancient *Platycladus orientalis*, 17 September 2023, Y. Zhang and N. Jiao (ZSCB7.1; living culture CGMCC3.27072). China, Beijing, Changping District, Ming Tombs, from blight leaf of ancient *P. orientalis*, 26 September 2023, Y. Zhang and N. Jiao (CLCB5.3; living culture CGMCC3.27066).

Notes: *Nothophoma spiraeae* was first reported as a plant pathogen causing canker disease from *Spiraea salicifolia* in Beijing, China (Zhang et al. 2020). In this study, two strains (CGMCC3.27066 and CGMCC3.27072) are clustered to the *N. spiraeae* clade in the combined phylogenetic tree (Fig. 1). Morphologically, the strains were similar to *N. spiraeae* revealed by conidia morphology (5.0–7.5 × 2.8–4.8 vs. 5.0–6.5 × 3.5–4.0 µm) (Fig. 3f, g). Therefore, we defined the isolated strains as *N. spiraeae*.

Nothophoma juglandis L. L. Zhao, W. Sun, L. Zhang, Y. Q. Yin, Y. Q. Xie, and Y. Zhang, Plant Disease, (2024) (Fig. 4).

Description: Conidiomata was pycnidial, semi-immersed or superficial on the agar surface, mostly aggregated, solitary or confluent. Pycnidia with age become black, appearing as small black spots, mostly globose to irregular, pale brown, dark brown near the ostioles, glabrous, thick-walled (Fig. 4a, b). Conidia are hyaline but incidentally olivaceous buff, ovoid, and blong to ellipsoidal, smooth and thin-walled, aseptate, 4.5–7.5 × 4.0–5.5 µm (mean SD = 5.0 ± 0.4 × 4.5 ± 0.5 µm, $n = 50$), sometimes with some very small guttules (Fig. 4f, g).

Culture characteristics: Colonies on MEA, 50 to 54 mm in diameter after 7 days at 26°C, margin regular. The aerial mycelium was flat, dark brown to black. The back side was pale brown to black, gradually darkening at 7 to 10 days. The colonies appeared dense and fluffy, with abundant pycnidia and irregular distribution on

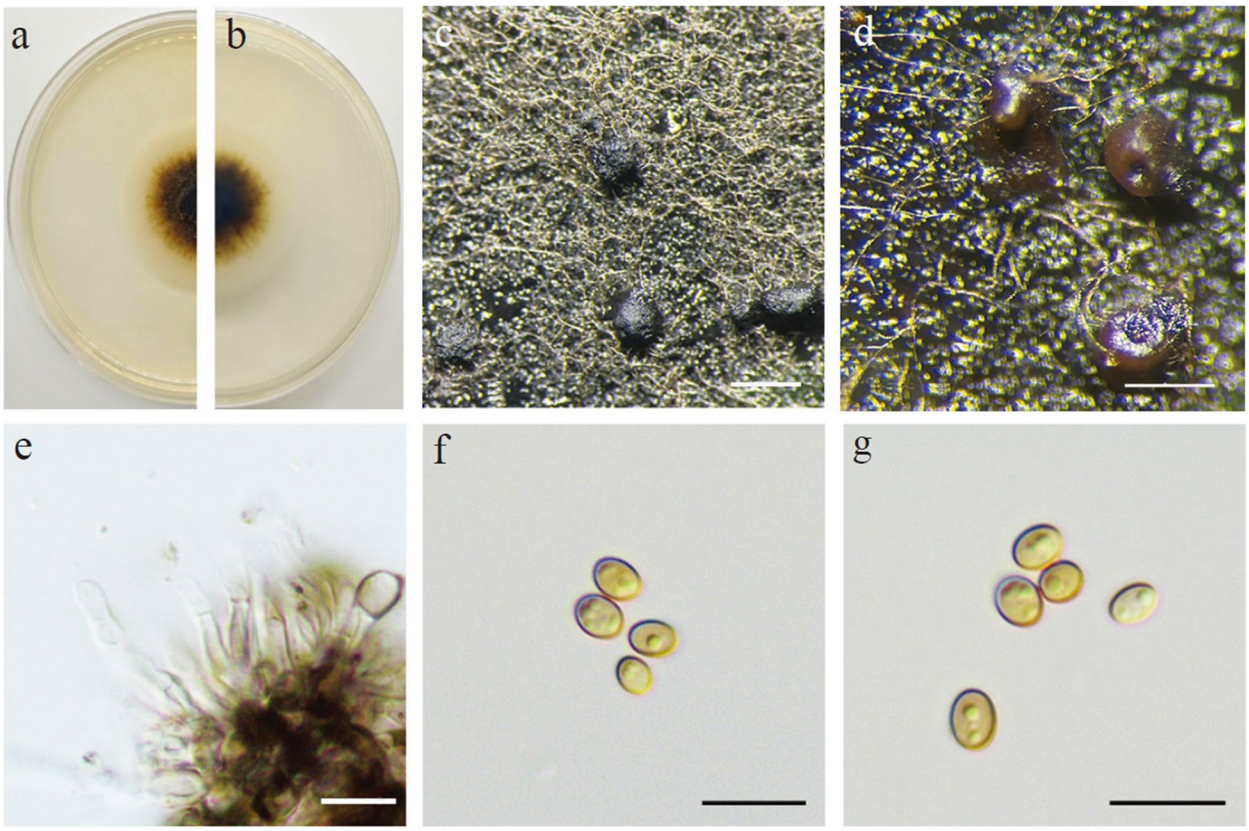

Fig. 2 Morphology of *Nothophoma platycladus* (CGMCC3.27070). **a**, **b** Colonies and reverse sides after seven days incubation on MEA. **c**, **d** Pycnidia were produced on the colony surface. **e** Conidiogenous cells. **f**, **g** Released conidia. Scale bars: 650 μm for **c**; Scale bars: 285 μm for **d**; Scale bars: 10 μm for **e**–**g**

the medium's surface, producing a conidial matrix drop (Fig. 4a, b).

Additional specimens examined: China, Beijing, Changping District, Ming Tombs, from blight leaf of ancient *Platycladus orientalis*, 26 September 2023, Y. Zhang and N. Jiao (CLCB2.3; living culture CGMCC3.27067). China, Beijing, Changping District, Ming Tombs, from blight leaf of ancient *P. orientalis*, 26 September 2023, Y. Zhang and N. Jiao (CLCB2.4; living culture CGMCC3.27068).

Notes: *Nothophoma juglandis* was first isolated from the branches of heart rot diseased walnut in Beijing, China (Zhao et al., 2024). In this study, two strains (CGMCC3.27067 and CGMCC3.27068) are clustered to the *N. juglandis* clade in the combined phylogenetic tree (Fig. 1). There is almost no difference in morphology and size of conidia between our strains and type specimen (4.5–7.5 × 4.0–5.5 vs. 5.0–8.0 × 4.0–6.0 μm) (Fig. 4f, g). Therefore, we identified the isolated strains as *N. juglandis*.

Pathogenicity test

There is no distinction in the symptoms of leaves infected by three *Nothophoma* species collected in the wild, and all are shown as symptoms in Fig. 5a. Three species of *Nothophoma* were performed for the pathogenicity testing on *P. orientalis* leaves. One week later, leaves inoculated with *Nothophoma* isolates have developed a yellow or brown necrotic blight at the inoculation site, with lesions gradually spreading towards the edge of the leaves (Fig. 5b–h). Pathological symptoms are similar to leaf blight spots collected in the wild, while all controls remained healthy (Fig. 5i, j). The pathogenicity assessment indicated that the length of lesions on leaves inoculated with mycelial plugs was significantly longer than that on un-inoculated leaves, and all tested strains exhibited similar pathogenic levels (Table 2). Koch's postulates were performed by successful pathogen re-isolation from all the necrotic areas of leaves. The morphology and DNA sequences of these new isolates were consistent with the initial inoculation.

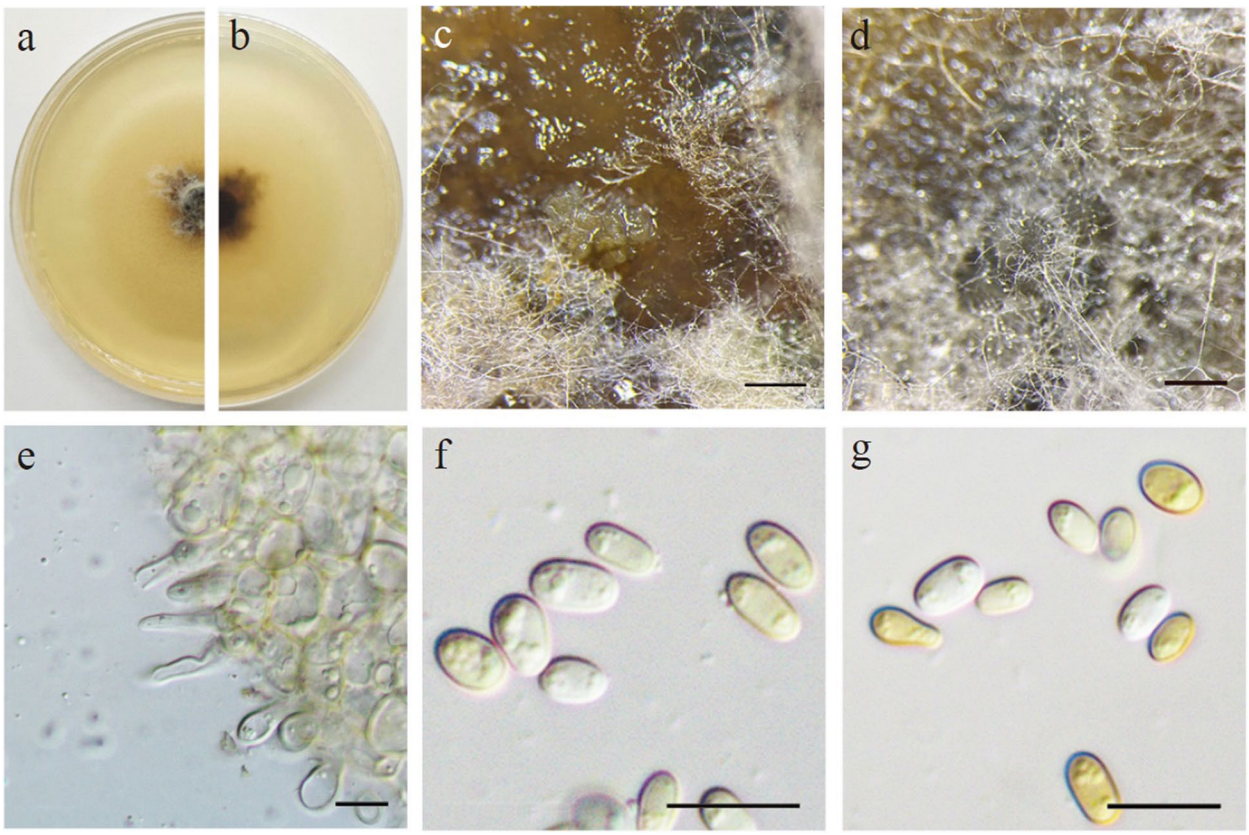

Fig. 3 Morphology of *Nothophoma spiraeae* (CGMCC3.27072). **a**, **b** Colonies and reverse sides after seven days incubation on MEA. **c**, **d** Pycnidia produced on the colony surface. **e** Conidiogenous cells. **f**, **g** Released conidia. Scale bars: 650 μm for **c**, **d**; Scale bars: 10 μm for **e**–**g**

Discussion

The genus *Nothophoma* was introduced by Chen et al. (2015) based on an independent evolutionary branch formed from five "*Phoma*" species (*Phoma anigozanthi*, *Phoma arachidis-hypogaeae*, *Phoma infossa*, *Phoma quercina*, and *Phoma gossypiicol*) in the Didymellaceae. Morphologically, *Nothophoma* was characterized that conidiomata pycnidial were immersed to superficial, solitary or confluent, and spherical to irregular. The pycnidial wall pseudoparenchymatous was composed of 3–6-layered isodiametric cells. The conidiogenous cells were phialidic, hyaline, smooth, ampulliform to doliiform, and producing aseptate conidia (Chen et al. 2015). The submmersed, solitary conidiomata, phialidicconidiogenous cells are hyaline, smooth, ampulliform to doliiform. The aseptate conidia point all these three isolated species to *Nothrophoma*.

Some species of *Nothophoma* have weak host specificity and can infect multiple plants and cause diseases. For example, *Nothophoma quercina* can cause leaf or branch diseases in various plants, including *Anacardiaceae*, *Fagaceae*, *Garryaceae*, *Oleaceae*, *Rhamnaceae*, *Rosaceae*, *Rhamnaceae*, and *Ulmaceae* (Hou et al. 2020; Wang et al. 2023). This species has been reported to cause leaf blight of *Magnolia coco*, and leaf spot of *Phellodendron amurense*, *Aucuba japonica*, and *Juglans regia* (Jiao et al. 2017; Lv et al. 2020; Zeng et al. 2021; Wang et al. 2023). In addition to angiosperms, *N. quercina* can also cause leaf blight in gymnosperms. A recent study on the dieback and decline of coniferous in Tbilisi (capital of Georgia) revealed that *N. quercina* caused leaf blight and branch dieback of local urban coniferous plantations, including *P. orientalis* (Danelia et al. 2021). This result proves that *Nothphoma* can infect the plants of Cupressaceae.

Based on the combined morphology with ITS, 18S rDNA, and *β-tubulin* phylogenetic analysis, *Alternaria alternata* and *Pestalotiopsis paeoniicola* were identified as the causal agents of leaf blight on ancient *P. orientalis* at the Mausoleum of the Yellow Emperor in Shaanxi Province. These pathogens can infect ancient *P. orientalis* either individually or in combination (Li et al. 2021). The diverse pathogenic fungi that infect the leaves of ancient *P. orientalis* are varied and different pathogens may act synergistically to produce complex pathogenic mechanisms. Revealing the pathogenic species of ancient *P. orientalis* leaf blight is a

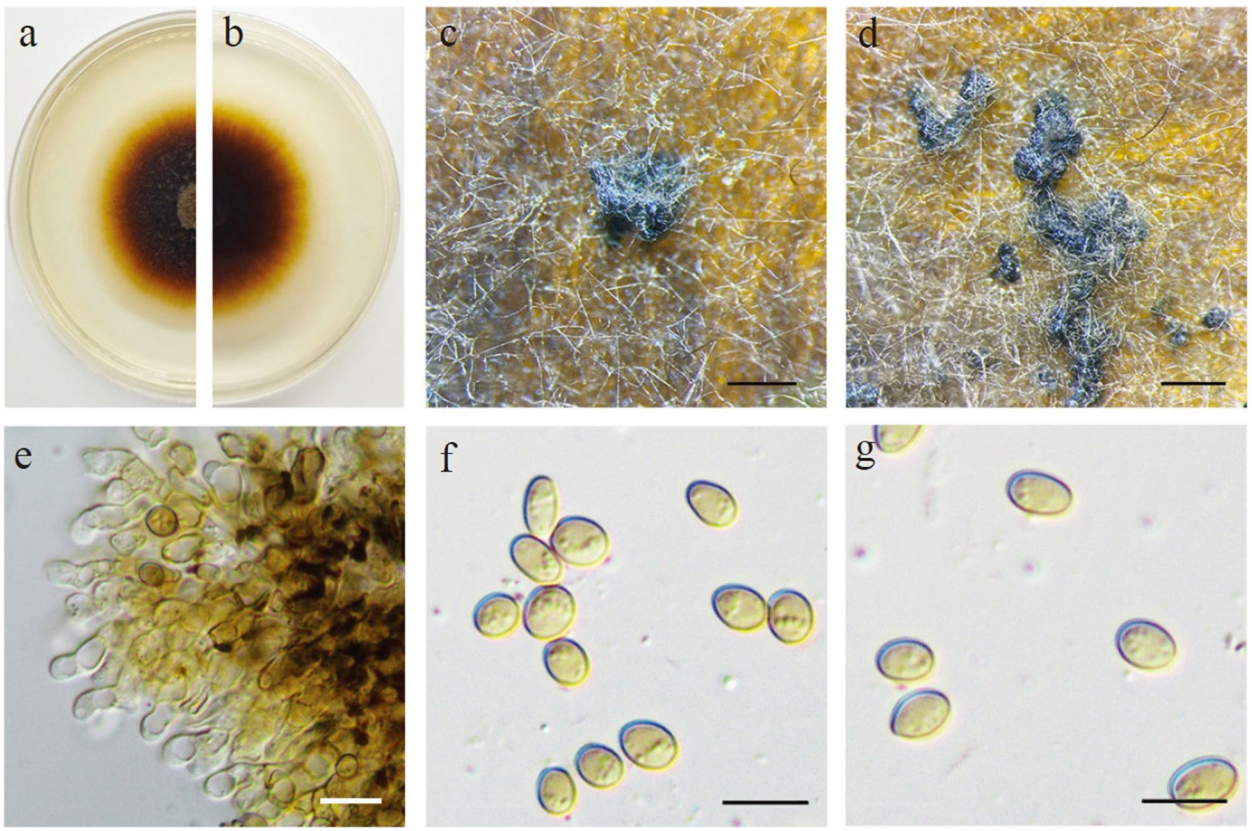

Fig. 4 Morphology of *Nothophoma juglandis* (CGMCC3.27068). **a**, **b** Colonies and reverse sides after seven days incubation on MEA. **c**, **d** Pycnidia produced on the colony surface. **e** Conidiogenous cells. **f**, **g** Released conidia. Scale bars: 650 μm for **c**, **d**; Scale bars: 10 μm for **e**–**g**

prerequisite for control. In this study, all these three species of *Nothophoma*, namely *N. platycladus*, *N. spiraeae*, and *N. juglandis*, cause leaf blight of ancient *P. orientalis* in Beijing, China, which is the first report of a species of *Nothophoma* causing disease on ancient cypresses.

Conclusion

In this study, we combined morphological and phylogenetic analysis to identify three *Nothophoma* species isolated from blight leaves of ancient *P. orientalis* in Beijing, namely *N. platycladus*, *N. spiraeae*, and *N. juglandis*. Pathogenicity testing revealed that all three species are the causal agents of leaf blight, with *N. platycladus* being recognized as a species new to science. The ancient *P. orientalis* leaf blight, caused by this three *Nothophoma* species mentioned above, was reported for the first time globally. Further studies require the collection of a large number of leaf samples to study the diversity of pathogenic fungi that can cause leaf blight of ancient *P. orientalis*.

Method

Sample collection and fungal isolation

A total of 26 blight leaf samples were collected from four locations in Beijing, China, in September, 2023 (11 samples from Zhongshan Park, 6 samples from Ritan Park, 5 samples from Beihai Park, and 4 samples from the Ming Tombs). Plant tissues ($0.5 \times 0.5 \times 0.2$ cm) were cut from the disease-healthy transition zone, then were surface sterilized with 75% ethanol for 30 s, rinsed 3 times with sterile distilled water, dried on sterilized filter paper and incubated on MEA for fungal strains (Soltani and Moghaddam 2014; Zhao et al. 2019). The petri dishes were incubated in the dark at 26°C until fungal colonies were observed. Pure cultures were obtained by hyphal tips from the margin of the suspected *Nothophoma* colonies, which were subcultured on fresh MEA and maintained at 26°C. A total of 20 *Nothophoma* strains were obtained. Based on colony features, conidial morphology, and *rpb*2 gene sequences, seven strains representing different tentative species and different locations were selected for further study (Table 1).

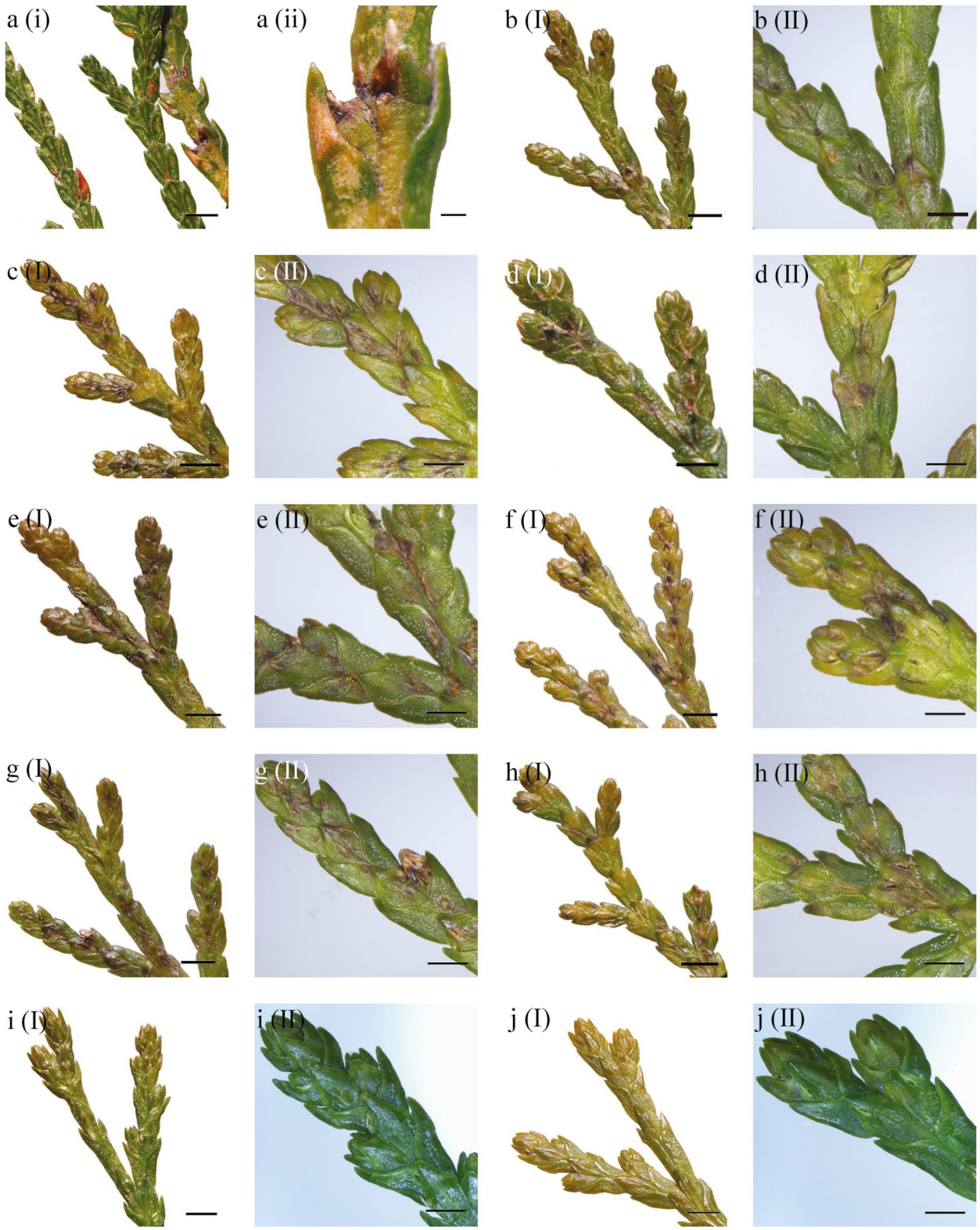

Fig. 5 Pathogenicity test of seven *Nothophoma* strains on *Platycladus orientalis* leaves. **a** (**i**, **ii**) Blight leaves collected in the wild. **b** (**I**, **II**)–**h** (**I**, **II**) Symptoms of *P. orientalis* leaves one week after inoculation with seven strains of *Nothophoma* (CGMCC3.27069, CGMCC3.27070, CGMCC3.27071, CGMCC3.27072, CGMCC3.27066, CGMCC3.27067, CGMCC3.27068 in order). **i**–**j** (**I**, **II**) control. Scale bars: 2 mm for **I**, **i**; Scale bars: 0.4 mm for **ii**; Scale bars: 1 mm for **II**

Table 2 Pathogenicity assessment of seven *Nothophoma* strains one week after inoculation on *Platycladus orientalis* leaves

Species	Number of strain	Origin	Number of sample	Mean length of necrotic lesions ± SD (mm)
Nothophoma platycladus	CGMCC3.27069	Ritan Park	RTCB 1–1	0.89 ± 0.18 a
	CGMCC3.27070	Ritan Park	RTCB 5–1	0.99 ± 0.22 a
	CGMCC3.27071	Beihai Park	BHCB 4–1	0.99 ± 0.14 a
Nothophoma spiraeae	CGMCC3.27072	Zhongshan Park	ZSCB 7–1	0.98 ± 0.26 a
	CGMCC3.27066	Ming Tombs	CLCB 5–3	1.01 ± 0.13 a
Nothophoma juglandis	CGMCC3.27067	Ming Tombs	CLCB 2–3	0.96 ± 0.22 a
	CGMCC3.27068	Ming Tombs	CLCB 2–4	0.90 ± 0.13 a
Non-inoculated control	/	/	CK	0 ± 0 b

Data followed by different letters in each column are significantly different, based on HSD tests at the $P < 0.05$ level

Morphological studies

To evaluate the colony characteristics, mycelial plugs in 8 mm diameter were transferred from the growing edges of 7-day-old colonies in new MEA dishes and incubated at 26°C under dark conditions (Liu et al. 2017). Following a week of incubation, black pycnidia were subsequently observed. Next, 1 mL of sterile water were added onto the face of each plate to release conidia from the pycnidia, and then collected for further measurements (Zou et al. 2021). The color, structure, and size of pycnidia were photographed, and at least 30 conidia were randomly selected for length and width measurement using a microscope (Nikon Eclipse E600) (Zhang et al. 2023). Fungal isolates and specimens were deposited at Beijing Forestry University (BJFU), with duplicates at the China General Microbiological Culture Collection Center (CGMCC) and the Mycological Herbarium of the Institute of Microbiology, Chinese Academy of Sciences (HMAS).

DNA extraction, PCR amplification, and sequencing

DNA was extracted from mycelia grown on MEA plates with CTAB plant genome DNA fast extraction kit (Aidlab Biotechnologies Co., Ltd, Beijing, China). The ITS region was amplified with the primers ITS1 and ITS4 (White et al. 1990), the *tub*2 region with primers Bt2a and Bt2b (Glass and Donaldson 1995), and the *rpb*2 region with primers *rpb*2-5F and *rpb*2-7cR (Liu et al. 1999). PCR amplification and sequencing followed the protocol of Zhang et al. (2009). PCR amplicons were purified and sequenced at BGI Tech Solutions (Beijing Liuhe) Co., Limited (Beijing, China).

Sequence alignment and phylogenetic analysis

DNA sequences of concatenated ITS, *rpb*2, and *tub*2 loci were analyzed to investigate the phylogenetic relationships among *Nothophoma* species with DNA sequences available from GenBank (http://www.ncbi.nlm.nih.gov/genbank/), as well as the sequences generated herein (Table 1). Multiple sequence alignment was performed by the MAFFT v.7.110 (http://mafft.cbrc.jp/alignment/server/). Ambiguous sequences at the start and the end were deleted and manually adjusted using BioEdit (Dania et al. 2021).

Maximum likelihood, Bayesian inference, and Maximum parsimony are used for the multi-locus analyses. Maximum likelihood analyses were constructed on the RAxML-HPC BlackBox 8.2.10 (Stamatakis 2014) using the GTR + GAMMA model with 1000 bootstrap replicates. Bayesian phylogenetic analysis was performed using a Markov Chain Monte Carlo (MCMC) algorithm in MrBayes v. 3.2.6 (Ronquist et al. 2012). Four MCMC chains were run from random trees for 2,000,000 generations and trees were sampled by each 1000th generation. The first 25% of the trees of MCMC sampling were discarded as burn-in and posterior probabilities (PP) were determined from the remaining trees. Maximum parsimony was conducted with heuristic searches as implemented in PAUP* v. 4.0b10 with the default options method (Swofford 2002). Ambiguous regions in the alignment were excluded and gaps were treated as missing data. Clade stability was evaluated in a bootstrap analysis with 1000 replicates with the Maxtrees set to 1000 and other default parameters implemented in PAUP* (Hillis and Bull 1993). Other measurements calculated parsimony scores including consistency index

(CI), retention index (RI), rescaled consistency (RC), and homoplasy index (HI). The phylogenetic trees were plotted using FigTree v.1.4.4 (http://tree.bio.ed.ac.uk/software/figtree) and edited using Adobe Illustrator CC2020 (Adobe Systems Inc., USA). New sequences generated in this study were deposited in GenBank (submission ID: 14366474, 2816058, and 2816060).

Pathogenicity test

Three identified species of *Nothophoma*, including their type and authentic isolates (seven selected isolates in total), were tested for their pathogenicity on detached living leaves of *P. orientalis*. Fresh and healthy leaves were collected from *P. orientalis* in Ritan Park on October 18, 2023. For pathogenicity testing, the leaves were washed with sterilized water and then surface sterilized with 75% ethanol for 1 min. Subsequently, mycelial plugs in 5 mm diameter cut from 7-day pure cultures of the isolates grown on MEA, and placed on the micro-wounds of leaves created with a sterile needle. Controls were treated with plugs cut from uninoculated MEA (Gomzhina and Gannibal 2023). Three leaves were included in per group, and the experiments were repeated three times. The inoculated leaves were incubated in sterile petri dishes under light at 12/12 h photoperiod, 26/22°C, as well as 80% relative humidity. Pathogenicity was determined by observing and measuring lesion length of the leaves after one week using stereomicroscope (OLYMPUS SZX7 and Nikon SMZ800N). Fungal isolates were re-isolated from the infected tissue, and morphological characterization and DNA sequence comparisons were conducted to fulfill Koch's postulates. Mean comparisons were conducted using Tukey's honest significant difference (HSD) test ($\alpha = 0.05$) in R (Version 3.2.2, R Inc. Auckland, NZL).

Abbreviations

BI	Bayesian inference
BJFU	Beijing Forestry University
CGMCC	China General Microbiological Culture Collection Center
CI	Consistency index
HI	Homoplasy index
HMAS	Mycological Herbarium of the Institute of Microbiology, Chinese Academy of Sciences
HSD	Honest Significant Difference
ITS	Internal transcribed spacer
MCMC	Markov Chain Monte Carlo
MEA	Malt extract agar
ML	Maximum likelihood
MP	Maximum parsimony
PP	Posterior probabilities
RC	Rescaled consistency
RI	Retention index
rpb2	RNA polymerase second largest subunit
tub2	β-Tubulin

Acknowledgements

Dr. Jinlong Zhang (Kadoorie Farm and Botanic Garden, KFBG) was acknowledged for assistance in the manuscript preparation.

Authors' contributions

YZ designed the research and revised the manuscript; NJ performed the research and wrote the manuscript; JW and ZZ conducted the sample collection for this study. All authors read and approved the final manuscript.

Funding

This work was supported by the National Natural Science Foundation of China (General Program) under grant numbers 31971658, 31770015, and 31370063 and the National Natural Science Foundation of China Projects of International Cooperation and Exchanges under grant number 3155461143028.

Availability of data and materials

Not applicable.

Declarations

Ethics approval and consent to participate

Not applicable.

Consent for publication

Not applicable.

Competing interests

The authors declare that they have no competing interests.

Received: 11 April 2024 Accepted: 15 June 2024
Published online: 24 September 2024

References

Abdel-Wahab MA, Bahkai AHA, El-Gorban AM, Hodhod MS. Natural products of *Nothophoma multilocularis* sp. nov. an endophyte of the medicinal plant Rhazya stricta. Mycosphere. 2017;8:1185–200. https://doi.org/10.5943/mycosphere/8/8/15.

Blicharska M, Mikusiński G. Incorporating social and cultural significance of large old trees in conservation policy. Conserv Biol. 2014;28:1558–67. https://doi.org/10.1111/cobi.12341.

Chen X. Diversity of Ancient Trees in Beijing. Sci Technol Eng. 2010;10:6623–7.

Chen Q, Jiang JR, Zhang GZ, Cai L, Crous PW. Resolving the *Phoma* enigma. Stud Mycol. 2015;82:137–217. https://doi.org/10.1016/j.simyco.2015.10.003.

Chen JQ. Health Assessment of Ancient Trees in Beijing. PhD Thesis, Beijing Forestry University, China. 2014.

Dai YS, Wang XD, Lin QR. Research on the pathogen of leaf blight of *Platycladus orientalis*. Journal of Nanjing Forestry University. 1992;16:59–65.

Danelia I, Zaqariashvili N, Amiranashvili L, Badridze G, Kvitsiani S. The mycological study of conifers in Tbilisi and its surroundings. J Forest Sci. 2021;67:464–76. https://doi.org/10.17221/79/2021-JFS.

Dania VO, Fajemisin AO, Azuh VO. Morphological and molecular characterization of *Aspergillus niger* causing postharvest rot of white yam (*Dioscorea rotundata* Poir). Arch Phytopathol Plant Protect. 2021;54:2356–74. https://doi.org/10.1080/03235408.2021.1983365.

Glass NL, Donaldson GC. Development of primer sets designed for use with the PCR to amplify conserved genes from filamentous ascomycetes. Appl Environ Microbiol. 1995;61:1323–30. https://doi.org/10.1128/aem.61.4.1323-1330.1995.

Gomzhina MM, Gannibal PB. First report of *Phyllosticta spinarum* causing arborvitae foliar blight in Russia. Forest Pathol. 2023;53:e12796. https://doi.org/10.1111/efp.12796.

Hillis DM, Bull JJ. An empirical test of bootstrapping as a method for assessing confidence in phylogenetic analysis. Syst Biol. 1993;42:182–92. https://doi.org/10.1093/sysbio/42.2.182.

Hou LW, Groenewald JZ, Pfenning LH, Yarden O, Crous PW, Cai L. The phoma-like dilemma. Stud Mycol. 2020;96:309–96. https://doi.org/10.1016/j.simyco.2020.05.001.

Huang L, Jin C, Zhou LH, Hu SW, Tian LJ, Li CQ, et al. Large old trees in human settlements: distribution patterns, drivers and conservation practices.

Guihaia. 2021;41:1665–73. https://doi.org/10.11931/guihaia.gxzw202108054.
Jiang JS, Tian Y, Zhang WY, Chen WF. Preliminary investigationon leaf blight of *Platycladus orientalis* in Hanwang Mountainforest farm of Yang County. Shaanxi Forestry Technol. 1984;3:11–3.
Jiao WL, Zhou RJ, Fu JF, Xu HJ, Hao N. First report of *Nothophoma quercina* causing leaf spot disease of *Phellodendron amurense* in China. Plant Dis. 2017;101:1820–1. https://doi.org/10.1094/PDIS-01-17-0079-PDN.
Li PQ, Ming J, Zhang SY, Yu ZD, He H, Tang GH. Pathogen identification and selection of controlling fungicides of leaf blight of *Platycladus orientalis* at the Mausoleum of Yellow Emperor. J Northwest A & F Univ (Nat Sci Edition). 2021;49:74–84. https://doi.org/10.13207/j.cnki.jnwafu.2021.01.009.
Li X, Chen X, Yuan W, Zhang X, Mao A, Zhao W, et al. Effects of *Platycladus orientalis* Leaf Extract on the Growth Performance, Fur-Production, Serum Parameters, and Intestinal Microbiota of Raccoon Dogs. Animals. 2023;13:3151. https://doi.org/10.3390/ani13193151.
Lindenmayer DB, Laurance WF. The ecology, distribution, conservation and management of large old trees. Ecol Conserv Manage Aspen Lit Rev. 2017;92:1434–58. https://doi.org/10.1111/brv.12290.
Liu YL, Whelen S, Hall BD. Phylogenetic relationships among ascomycetes: Evidence from an RNA polymerase II subunit. Mol Biol Evol. 1999;16:1799–808. https://doi.org/10.1093/oxfordjournals.molbev.a026092.
Liu LP, Yan YQ, Huang JB, Hsiang T, Wei YD, Li Y, et al. A Novel MFS Transporter Gene *ChMfs1* Is Important for Hyphal Morphology, Conidiation, and Pathogenicity in *Colletotrichum higginsianum*. Front Microbiol. 2017;8:e1953. https://doi.org/10.3389/fmicb.2017.01953.
Liu JJ, Lindenmayer BD, Yang WJ, Ren Y, Campbell MJ, Wu CP, et al. Diversity and density patterns of large old trees in China. Sci Total Environ. 2019;655:255–62. https://doi.org/10.1016/j.scitotenv.2018.11.147.
Lv YC, Yang CL, Liu YG, Zeng Q, Liu SY, Zhu TH, et al. First report of leaf blight on *Aucuba japonica* caused by *Nothophoma quercina* in China. Plant Dis. 2020;104:2731–2731. https://doi.org/10.1094/PDIS-01-20-0201-PDN.
Ronquist F, Teslenko M, van der Mark P, Ayres DL, Darling A, Höhna S, et al. MrBayes 3.2: Efficient bayesian phylogenetic inference and model choice across a large model space. Syst Biol. 2012;61:539–42. https://doi.org/10.1093/sysbio/sys029.
Soltani J, Moghaddam MSH. Antiproliferative, Antifungal, and Antibacterial Activities of Endophytic *Alternaria* Species from Cupressaceae. Curr Microbiol. 2014;69:349–56. https://doi.org/10.1007/s00284-014-0594-8.
Stamatakis A. RAxML version 8: A tool for phylogenetic analysis and post-analysis of large phylogenies. Bioinformatics. 2014;30:1312–3. https://doi.org/10.1093/bioinformatics/btu033.
Swofford DL. PAUP*: phylogenetic analysis using parsimony (*and other methods). Version 4.0b10. Sinauer Associates, Sunderland, Massachusetts. 2002.
Wan JZ, Li QF, Wei GL, Yin GJ, Wei DX, Song ZM, et al. The effects of the human footprint and soil properties on the habitat suitability of large old trees in alpine urban and periurban areas. Urban Forestry Urban Greening. 2020;47:126520. https://doi.org/10.1016/j.ufug.2019.126520.
Wang FH, Liu C, Zeng Q, Zhou YJ, Liu F, Xu XL, et al. Identification and pathogenicity analysis of leaf brown spot of *Juglans regiain* in China. Sci Rep. 2023;13:6599. https://doi.org/10.1038/s41598-023-33853-1.
White TJ, Bruns T, Lee S, Taylor JL. Amplification and direct sequencing of fungal ribosomal RNA genes for phylogenetics. PCR Protocols Guide Methods Appl. 1990;18:315–22. https://doi.org/10.1016/B978-0-12-372180-8.50042-1.
Zeng Q, Lv YC, Li XY, Xu XL, Yang CL, Deng Y, et al. Leaf blight of *Magnolia coco* caused by *Nothophoma quercina* in China. Plant Dis. 2021;106:761. https://doi.org/10.1094/PDIS-05-21-1061-PDN.
Zhang Y, Wang HK, Fournier J, Crous PW, Jeewon R, Pointing SB, et al. Towards a phylogenetic clarification of *Lophiostoma/Massarina* and morphologically similar genera in the Pleosporales. Fungal Divers. 2009;38:225–51. https://doi.org/10.1002/yea.1704.
Zhang LX, Yin T, Pan M, Tian CM, Fan XL. Occurrence and identification of *Nothophoma spiraeae* sp. nov. in China. Phytotaxa. 2020;430:147–56. https://doi.org/10.11646/phytotaxa.
Zhang L, Yin YQ, Zhao LL, Xie YQ, Han J, Zhang Y. Two new species of *Colletotrichum* (Glomerellaceae, Glomerellales) causing walnut anthracnose in Beijing. MycoKeys. 2023;99:131–52. https://doi.org/10.3897/mycokeys.99.106812.
Zhao HQ. Garden disease and pest control. Beijing: China Architecture and Building Press; 1978. p. 183–4.
Zhao L, Cai J, He W, Zhang Y. *Macrophomina vaccinii* sp. nov. causing blueberry stem blight in China. MycoKeys. 2019;55:1–14. https://doi.org/10.3897/mycokeys.55.35015.
Zhao LL, Sun W, Zhang L, Yin YQ, Xie YQ, Zhang Y. Heart rot disease of walnut caused by *Nothophoma juglandis* sp. nov. and its endophytic biocontrol agent. Plant Disease. 2024;108(3):746–56. https://doi.org/10.1094/PDIS-11-22-2660-RE.
Zheng CY, Zhou QA, Shao WQ, Zhang J, Wang J. Early identification of fungal leaf blight disease (*Alternaria alternate*) on *Platycladus orientalis* plants by using gas chromatography-ion mobility spectrometry. Microchem J. 2022;179:107505. https://doi.org/10.1016/j.microc.2022.107505.
Zhu FM. A new disease of cypresses: leaf inflammation. J Chin Agric Soc. 1922;33:21–9.
Zou J, Dong YH, Wang HZ, Liang WX, Li DL. Identification and Characterization of *Nothophoma quercina* Causing Bud Blight on *Photinia* × *fraseri* in China. Plant Dis. 2021;105:1356–64. https://doi.org/10.1094/PDIS-06-20-1218-RE.